Celastrol Exerts Neuroprotective Effect via Directly Binding to Hmgb1 Protein in Cerebral Ischemic Reperfusion

Dandan Liu
China Academy of Chinese Medical Sciences Institute of Chinese Materia Medica
Piao Luo
China Academy of Chinese Medical Sciences Institute of Chinese Materia Medica
Liwei Gu
China Academy of Chinese Medical Sciences Institute of Chinese Materia Medica
Qian Zhang
China Academy of Chinese Medical Sciences Institute of Chinese Materia Medica
Peng Gao
China Academy of Chinese Medical Sciences Institute of Chinese Materia Medica
Yongping Zhu
China Academy of Chinese Medical Sciences Institute of Chinese Materia Medica
Xiao Chen
China Pharmaceutical University
Junzhe Zhang
China Academy of Chinese Medical Sciences Institute of Chinese Materia Medica
Nan Ma
China Academy of Chinese Medical Sciences Institute of Chinese Materia Medica
Jigang Wang (jgwang@icmm.ac.cn)
China Academy of Chinese Medical Sciences Institute of Chinese Materia Medica
https://orcid.org/0000-0002-0575-0105

Research Article

Keywords: celastrol, chemical proteomics, target identification, high mobility group protein 1, cerebral ischemic reperfusion

Posted Date: April 16th, 2021

DOI: https://doi.org/10.21203/rs.3.rs-412365/v1

Version of Record: A version of this preprint was published at Journal of Neuroinflammation on August 9th, 2021. See the published version at https://doi.org/10.1186/s12974-021-02216-w.

Abstract

Background: Celastrol is one of the early isolated and identified chemical constituents from *Tripterygium wilfordii* Hook.f.. Based upon the celastrol probe that maintained the bioactivity of the parent compound, the targets of celastrol in cerebral ischemic reperfusion (I/R) were comprehensively analyzed by quantitative chemical proteomics method.

Methods: We constructed primary cortical neurons model of oxygen-glucose deprivation (OGD) and rat model of middle cerebral artery occlusion (MCAO) to detect the targets of celastrol in cerebral I/R. Combining with various experimental methods such as tandem mass tags (TMT) labeling, mass spectrometry and cellular thermal shift assay (CETSA), we revealed the directly binding cellular targets of celastrol.

Results: We uncovered that celastrol inhibited pro-inflammatory activity of high mobility group protein 1 (HMGB1) by directly binding to it and then blocking the binding of HMGB1 to its inflammatory receptors in the microenvironment of ischemic and hypoxia. In addition, celastrol rescued neurons from OGD injury *in vitro* and decreased cerebral infarction *in vivo* by targeting HSP70 and NF-κB.

Conclusion: Celastrol exhibited neuroprotective and anti-inflammatory effects via targeting HSP70 and NF-κB and directly binding to HMGB1 in cerebral ischemic reperfusion injury.

Background

Tripterygium wilfordii Hook. f. (*Tw*HF)-based prescription is widely used in the treatment of autoimmune diseases, tumor and so on in China for centuries [1, 2]. Out of many bioactive constituents isolated from *Tripterygium wilfordii*, celastrol has attracted closed attention for more than 70 years in terms of possible medicinal property [3]. Celastrol exhibits a diversity of pharmacological effects in a wide range of disorders, such as cancer, diabetic, obesity [4], neurodegenerative diseases [3]. An abundance of existing researches have proved neuroprotective effects of celastrol in neurodegenerative diseases through anti-oxidant and attenuating neuro-inflammation [5]. Besides, celastrol excellently relieved acute ischemic stroke-induced injury by promoting microglia/macrophage M2 polarization [6], reducing the expressions of p-JNK, p-c-Jun and NF-κB [7], and inhibiting high mobility group box 1 (HMGB1)/NF-κB signaling pathway to exhibit anti-inflammatory and antioxidant actions in transient global cerebral ischemic rats [8]. However, there are few studies about whether celastrol has neuroprotection effect for cerebral ischemic-reperfusion (I/R) injury and specific binding protein targets.

Neuro-inflammatory processes have been implicated in the pathophysiology of multiple stages of cerebral I/R injury, and targeting neuro-inflammation has always been an attractive treatment in stroke [9]. It has taken several periods for the intensive study of HMGB1 in inflammation related diseases, which is currently one of the crucial pro-inflammatory alarmin of stroke. The non-histone DNA binding protein HMGB1 is primarily located in the cell nucleus and behaves different biological functions according to cellular locations, binding receptors and redox states. HMGB1 shifts to the cytoplasm and extracellular

space by activated immune cells or passively released by necrotic or damaged cells, with dynamic redox states due to distinct posttranslational modifications [10] and activated inflammatory immune reaction [11]. Outside of the cell, HMGB1 serves as a damage-associated molecular pattern (DAMP) or alarmin to mediate inflammation through receptors including advanced glycation end products (RAGE), toll like receptor 2 and 4 (TLR2, TLR4) [12]. HMGB1 constitutes three domains: A box, B box (positively charged) domains and carboxyl terminus (negatively charged) acidic tail. The three cysteines located at positions 23, 45 (A box) and 106 (B box) mainly determine the redox state and physiological functions of HMGB1. The fully reduced HMGB1 only possesses chemotaxis by binding to CXCL12, and stimulates immune cell infiltration through the CXCR4 receptor in a collaborative way. An intramolecular disulfide bond of HMGB1 in cysteines C23 and C45 with critical C106 in a reduced state has pro-inflammatory activity like cytokines via the TLR4/MD-2 complex, induces nuclear NF-κB translocation and produces tumor necrosis factor (TNF) in macrophages. Meanwhile, chemotactic and cytokine activities disappeared after all the cysteines oxidized (sulfonyl HMGB1) [13, 14]. Therefore, disulfide HMGB1 isoform is a biomarker of inflammation and blocking extracellular disulfide HMGB1 isoform maybe a potential direction for the treatment inflammation and immune diseases, including stroke.

Quantitative chemical proteomics technology based on small molecule compound probe and chemical labeling has been widespread used for seeking targets and elucidating the mechanism of natural and traditional medicines [15], including Artemisinin [16], andrographolide [17], curcumin [18], aspirin [19]. With the help of activity-based celastrol probe (cel-p), tandem mass tags (TMT) labeling, liquid chromatography-tandem mass spectrometry (LC-MS/MS) and cellular thermal shift assay (CETSA), we elucidated the neuroprotective mechanism and targets of celastrol on stroke I/R injury, and uncovered that celastrol directly bond with HMGB1 to inactivate its cytokine activity and targeted HSP70 and NF-κB to exert anti-inflammatory activity.

Materials And Methods

Animals

All experiments were carried out for the sake of minimizing the number and suffering of animals. All experiments animal operations meet the requirements of the Beijing Administration Rule of Laboratory Animal, and were approved by the Animal Experimental Ethics Review Committee of the Institute of Basic Research for Chinese Medicine, China Academy of Chinese Medical Sciences.

The Sprague–Dawley rats within 12h of birth (Vital River Laboratories, Beijing, China) were used for primary cortical neurons isolation. Male Sprague–Dawley rats (260–280g, Vital River Laboratories, Beijing, China) used for middle cerebral artery occlusion (MCAO) experiment were housed in standard breeding environment without restriction to diet and drinking.

Reagents

Cell culture reagents: Dulbecco's modified Eagle medium (DMEM); Sugar free DMEM; DMEM/F-12 (1:1) and fetal bovine serum (FBS) were obtained from Corning, USA. Neurobasal-A medium; 50 × B27 supplement; 100 × penicillin-streptomycin (PS); 100 × Glutamax-I and 0.25% trypsin were purchased from Gibco, USA.

Click chemistry, pull down and LC-MS/MS reagents: NaVc; CuSO4; TAMRA Azide and Biotin-azide were obtained from Sigma, USA. High capacity neutravidin agarose resin; sequencing grade modified Trypsin; TMT 10 plex reagent set; TEAB and Pierce™ Quantitative Fluorometric Peptide Assay Kit were purchased from Thermo Fisher Scientific, USA. Oasis HLB Extraction Cartridge was obtained from Waters. THPTA was obtained from Click Chemistry Tools.

Other reagents: celastrol (HPLC >98%); edaravone injection (Yangtze River Pharm; China); recombinant human HMGB1 protein (Abcam, United States); Cell Counting Kit-8 (CCK-8; DOJINDO; Japan); Coomassie brilliant blue (CBB; Beyotime; China). For intraperitoneal injection (i.p.), celastrol was dissolved in 1% dimethylsulfoxide (DMSO) and 0.9% physiological saline in order to yield a concentration of 1 mg/3 ml. All other reagents were purchased from Thermo Fisher or Sigma without special instructions.

Rat primary cortical neurons isolation and RAW 264.7 cell culture

The neonatal Sprague–Dawley rats within 12h of birth were used for primary cortical neurons isolation as previously established with minor revise [20]. Briefly, the cortex of newborn rats was sterile separated in pre-cooling (4°C) DMEM/F-12 (1:1). The minced cortex tissue was digested with 0.2mg/ml DNase Ⅱ and 2mg/ml papain, and inactivated by adding 10% volume FBS. The cell suspension was washed twice with DMEM/F-12 (1:1) and re-suspended in DMEM/F-12 (1:1) containing 10% FBS and 1 × PS. The cells suspension passed through 300 mesh sieves were seeded on L-polylysine pre-coated orifice plate or dish and incubated at 37°C incubator with 5% (v/v) CO_2. 4-6h later, the DMEM/F-12 (1:1) was replaced with complete Neurobasal-A medium replenished with 1× PS, 1× Glutamax-I and 1× B27. The culture medium was change half every 2-3 days, and all the experiments were carried out on the seventh day unless otherwise stated.

RAW 264.7 cell was cultured in DMEM containing 10% FBS, 1× PS and maintained in a cell incubator. Cells were passage every 2-3 days and TNF-α was testing in cell within 20 passages.

Oxygen glucose deprivation (OGD) insult

The transient OGD model was constructed to simulate cerebral I/R injury in cultured primary neurons as previously described [21]. Briefly, the Neurobasal-A medium was displaced with deoxygenated, sugar free DMEM, and the cells were incubated in a hypoxia chamber (STEMCELL Technologies, Canada) filled with 95% N_2 + 5% CO_2 for 4 h in 37°C incubator and returned to normal culture condition according to the experimental requirement. In contrast, control cells were cultured in normal culture conditions. After reaching the established time, cell viability evaluation was determined by CCK8 assay or cells were

collected for other experiments. For CCK8 assay, absorbance was measured using a multimode plate reader (PerkinElmer, USA) at 450 nm.

Proteome reactivity profiles of primary neuron treated with cel-p

Fluorescence labeling profiling of cel-p binding proteins was conducted in living primary neuron with or without celastrol competitor and OGD model refer to previous operation [22]. Similarly, increasing concentrations of cel-p (0-1.6 μM) or cel-p (0.8μM) + competitor (celastrol 2 ×, 4 ×, 6 ×, 8 ×) were added into the 6 well plates with or without OGD interfere and incubated for 4 h in cell incubator. Then supernatant of cell lysate were collected and BCA method was used for protein concentration quantification. The click chemistry reaction was conduct with NaVc (100 mM stock solution, final concentration 1 mM), THPTA (100 mM stock solution, final concentration 100 μM), CuSO4 (100 mM stock solution, final concentration 1 mM) and TAMRA Azide (5 mM stock solution, final concentration 50 μM) in equal amounts (100 μg) of extracted protein for 2h at room temperature. The protein was precipitated with 1 ml pre-cooling (-20°C) acetone, and re-dissolved with 30 μl 1× SDS loading buffer. 15 μl of sample was separated with 10% sodium dodecyl sulfate-polyacrylamide gel electrophoresis (SDS-PAGE) gel, and the labeling profiles were visualized with in-gel fluorescence scanning in laser scanner (Azure Sapphire RGBNIR, USA) and then the gel was stained with CBB.

Cellular imaging of cel-p

Cellular imaging experiment was conduct with fluorescence microscopy as described previously to verify the utility of cel-p for imaging of potential cellular targets [23]. To track the cellular distribution of cel-p, living primary neurons were incubated with 0.8 μM cel-p for 0-6 h. The cells were fixed with 4% paraformaldehyde solution for 10 min and 0.2% Triton-X 100 permeated 15 min. Click chemistry reaction was carry out (regents and concentration referenced 2.3.3) for 2h and washed thrice to remove excessive agents. The nuclei were stained with Hoechst for 10min. The images were obtained with confocal fluorescence microscopy (Leica TCS SP8 SR, Germany).

Pull down, TMT labeling and targets validation

Pull-down, TMT labeling and LC-MS/MS experiments were carried out to identify the interacting cellular targets of celastrol and primary neuron according to previous description with certain modification [24]. Primary neuron cells cultured in 100 mm dishes were divided into the following groups and continue incubated for 4 h : Control (less than 1% DMSO), cel-p (4 μM), and celastrol 8 × (cel-p 4 μM + celastrol 32 μM). Click chemistry reaction was conduct with Biotin-azide (50 mM stock solution, final concentration 50 μM), NaVc, THPTA and CuSO4 (concentration referenced 2.3.3) in equal amounts (1 mg) of extracted protein from each sample for 4 h. The protein was precipitated in pre-cooling (-20°C) acetone, and re-dissolved with 0.1% SDS in PBS. The sample supernatants were poured into the washed agarose resin (50μl of agarose resin in each group) and incubated with gentle rotation for 4 h to make resin capture the biotinylated proteins.

For on agarose resin digestion, the agarose resin was washed thrice with 1% SDS, 0.1 % SDS and 6 M urea in order. The agarose resin was reduced with 6M urea and 100 mM Dithiothreitol (DTT) for 30 minutes. Then the cysteines were blocked with 6M urea and 400 mM IAA and incubated avoid from light for 45 minutes. 2μg trypsin was add into each sample and incubated overnight to digest the proteins captured on the agarose resin. Supernatant containing digestive peptides were separated from the mixture by centrifugation and loaded onto the activated Extraction Cartridge, and then the samples were transferred to a new tube spin dry. The dried samples were re-constituted with 100 mM TEAB, and the digestive peptides were subjected to TMT labeling subsequently on the basis of instructions. TMT 126C and 131N labeled for negative control samples 1 and 2, TMT 127C and 127N labeled for cel-p pull-down samples 1 and 2, TMT 130C and 130N labeled for celastrol 8 × pull-down samples 1 and 2. The labeling reaction was quenched 2 h later with 1M Tris HCl and the labeled samples were converged to a single new tube for LC-MS/MS (Thermo Fisher, Orbitrap Fusion Lumos, USA) identify and quantify.

Cellular Thermal Shift Assay (CETSA)

Target engagement assay of celastrol with HMGB1 was performed the same with previous article with minor modify [25]. The primary neurons in 100 mm dishes were collected with PBS containing protease inhibitor. The cells were subjected to freezing and thawing cycles in liquid nitrogen and repeated mechanical crushing to obtain cell lysate supernatant by centrifugation. Then equivalent supernatant (1 mg) was treated with either DMSO or celastrol (20 μM) 1h at room temperature with gently shaking. The treated supernatant was divided into ten equal parts and heated according to designated temperatures. The cooled samples were centrifugation again to obtain supernatant and conducted Western blot analysis.

Western blot analysis

Supernatants of neuron lysate or rat cerebral cortex tissues lysate were obtained with RIPA lysate and protease inhibitor. For the cytoplasm and nuclear protein extraction, the nuclear-cytosol extraction kit was used on the basis of instructions. Fully reduced and disulfide bond HMGB1 isoforms were detected in rat primary cortex neuron and condensed culture supernatant with non-reducing PAGE gel, and samples were collected avoid from reducing agent (β-mercaptoethanol or DTT). After OGD and celastrol treatments as detailed above, the culture supernatant was collected at 0, 4, 8, 12, 24, 48 h and centrifuged to discard cell debris. Then the supernatant was concentrated 20 folds with Amicon Ultra-4 50kDa and Amicon Ultra-4 10kDa. Protein content was identified using the BCA assay, and the denatured sample was separated with 10%, 12% or 15% SDS-PAGE gel.

Separated protein samples were transferred onto PVDF membranes, blocked in 5% bovine serum albumin (BSA)and incubated overnight at 4°C with anti-HMGB1, anti-HSP70, anti-NF-κB, anti-RAGE, anti-TLR4, PCNA, or β-actin primary antibody and then secondary antibodies (goat anti-rabbit, 1:5000; goat anti-mouse, 1:5000) for 2 h at room temperature. Membranes were washed thrice with TBST after incubation. The bands were visualized with enzyme-linked chemiluminescence in the detection system (Azure C400, USA).

Immunofluorescence staining

For animal Immunofluorescence, after series dewaxing and dehydration, rat cerebral cortex paraffin slice were incubated in antigen retrieval for 10 min in 95°C and permeabilized 15 min in 0.2% Triton X-100. The slices were blocked 1h in 5%BSA, incubated with primary antibodies against HMGB1, HSP70, or NF-κB at 4 °C overnight and 2 h with secondary fluorescence antibodies (goat anti-rabbit, 1:500; goat anti-mouse, 1:500, Abcam) avoiding from light. After 10 min of Hoechst staining, the slices were photographed with laser scanning confocal microscope.

For cell Immunofluorescence, the treated cells were washed with PBS, fixed in 4% paraformaldehyde solution and permeabilized in 0.2% Triton-X 100. The rest procedures were the same with animal Immunofluorescence.

Expression and purification of HMGB1 A box and B box

Recombinant human HMGB1 box A (residues 1–89) and box B (residues 90–175) were cloned in a modified pET-24d vector (Novagen, Madison, WI) expressing a protein with an N-terminal 6-His tag. The E. *coli* BL21 was transformed with pET24d-HMGB1 A box and pET24d-HMGB1 B box, cultured in LB medium containing 50g/ml kanamycin at 37℃ to an absorbance of 0.8 at 600 nm, and expression was induced with 0.4 mM Isopropyl-D-1-thiogalactopyranoside (IPTG) for 12h at 16℃ before being harvested by centrifugation. Cell pellets were suspended in lysis buffer (20 mM Tris-HCl, pH 8.0, 200mM NaCl, 1mM PMSF) and disrupted by sonication. After centrifugation (12000 g, 30 min, 4℃), the supernatant incorporated His-tagged recombinant A box or B box was applied to a Ni-beads column. The column was washed with 30 ml binding buffer (20 mM Tris-HCl, pH 8.0, 200 mM NaCl and 20 mM or 50 mM Imidazole). A box protein was eluted with elution buffer (20 mM Tris-HCl, pH 8.0, 200 mM NaCl and 200 mM Imidazole). B box protein was eluted with elution buffer (20 mM Tris-HCl, pH 8.0, 200mM NaCl and 100 mM Imidazole). The samples were exchanged by the buffer containing 20 mM Tris-HCl, pH 8.0, 200 mM NaCl and concentrated by using centrifugal filter units according to the protocol provided by manufacturer. The concentration of purified proteins was determined with BCA protein assay reagent kit. The purity and integrity of purified HMGB1 A box and B box was verified by CBB after 15% SDS-PAGE gel separation.

HMGB1 full-length, A box and B box labeling and activity assay

Briefly, recombinant human HMGB1 full-length protein, A box and B box were dissolved or diluted with PBS, and reacted with celastrol, cel-p, IAA, IAA-yne, Glycyrrhetinic acid (GA), Melatonin (Mel) or DTT as needed for a period of time. Subsequently, the click chemistry reaction was conducted as same with title 2.3.3 fluorescence labeling and the protein was separated with 12% (HMGB1 full-length protein) or 15% SDS-PAGE gel (A box and B box). The labeling state was visualized by i fluorescence laser scanner and stained with CBB.

For activity assay of celastrol and HMGB1 protein, recombinant human HMGB1 protein and celastrol combined HMGB1 activity were measured by stimulating TNF-α in RAW 264.7 cells for 24h. For confirming whether celastrol blocked the binding of receptors TLR4 and RAGE to B box, the semi *in vivo* precipitation of B box complex experiment was conduct as previously with minor revise [26]. 100 μg B box proteins were first reacted with or without equivalent amount (equimolar with B box, 10^{-2}μmol) and five folds amount of celastrol (5×10^{-2}μmol) in Ni-beads column for 1 h. Then 500 μg lysate of primary neurons was add into the Ni-beads column and reacted 2 h at 4a, and eluted to precipitate B box complex. The denatured complex sample was subjected to immunoblot analysis with antibodies against TLR4 and RAGE. The same B box with equivalent amount of celastrol elution did not incubate with cell lysate was used for TNF-α analysis in RAW 264.7 cells to research whether celastrol reduced the ability of B box inducd TNF-α secretion.

Induction of MCAO and neurological defect assessment in rats

By inserting an filament to occlude the right middle cerebral artery (MCA) of male Sprague–Dawley rats (250–280g), we established cerebral I/R model *in vivo* as described previously [27]. Briefly, the rats fasted overnight were anesthetized with continuous supply of 3% isoflurane + 95% oxygen mixture. A 4-0 monofilament was inserting into the internal carotid artery through a tiny incision in the external carotid artery to block the cerebral blood flow of MCA. 90 min later, the filament was withdrawn to resume blood stream providing. The Sham group did the same steps without inserting the filament. Four groups included: (1) Sham group, saline i.p.; (2) Model (M) group, saline i.p.; (3) M + cel 1mg/kg, i.p.; (4) M + eda 6 mg/kg, i.v..

The neurological deficits of rats were assessed at 24, 48, 72 h after reperfusion respectively by an experimenter who was blinded to the group information. Zea-Longa five-point scores was used to assess neurologic deficits according to previous description [27]. The animals without symptoms of neurological impairment or dying after surgery were rejected. 72h after reperfusion, infarct volume was determined by 2, 3, 5-triphenyltetrazolium chloride (TTC) stating and calculated with Image J software as previously [27]. Nissl-stained cells in the rat cerebral cortex were observed at 200 × magnifications with a light microscope to assess Nissl body damage.

Statistical analysis

Data were presented as the mean ± SEM. Raw data were statistically analyzed with Graph Pad Prism 5.0. The density of Westren blot bands was quantified using Image J software. The data were analyzed using one-way ANOVA. Fisher's least-significant difference post hoc test was used to test the differences between two groups. P value less than 0.05 was considered statistically significant.

Results

Celastrol and cel-p showed similar neuroprotective effect *in vitro*

Cel-p was synthesized with an alkynyl handle to the carboxyl terminal of celastrol (Fig. 1A). We first detected the cytotoxicity of celastrol and cel-p in living primary neuron. As shown in Fig. 1B, the IC_{50} results suggested that cel-p closely mimicked the original compound in biological activity (celastrol IC_{50} = 2.2 μM, cel-p IC_{50} = 2.0 μM). For cell viability assay, primary neurons were incubated in 96 well plates for 7 d and then experienced OGD model to evaluate the neuroprotective effect of celastrol and cel-p. As shown in Fig. 1C, celastrol exhibited obvious neuroprotective effect on the OGD model of primary neurons. The optimal dose of celastrol was 0.1-0.8 μM, and the optimal administration time was 48 h after OGD model. Cel-p showed similar neuroprotective effect with celastrol (Fig. 1D). Therefore, celastrol remained biological activity after introducing biorthogonal reaction groups and cel-p could be used to instead the celastrol for subsequent research.

Celastrol significantly decreased pathological changes of MCAO rats

Previous researches indicated that celastrol reduced neurological deficit, brain water content and infarct volume in rat permanent cerebral ischemic model [6, 7]. Therefore, we mainly evaluated whether celastrol exhibited neuroprotective effect for rat cerebral I/R injury. At 72 h after MCAO model, celastrol (1mg/kg, i.p.) significantly decreased the infarct volume (Fig. 2A, B), improved behavior indexes (Fig. 2C) and reduced cortex pathological changes of Nissl staining (Fig. 2D, E) of MCAO rats compared with Model group. The neuroprotective effect of celastrol was similar to positive control edaravone injection (6mg/kg, i.v.).

Cel-p possessed high bioconjugation efficiency

We evaluated the labeling profiles of cel-p in living primary neurons. As shown in Fig. 3A, cel-p showed strong labeling efficiency and concentration dependent labeled living primary neurons protein and produced obvious visible bands at as low as 0.8 μM probe concentration in 4 h of incubation time. As shown in Fig. 3B, the labeling profiles of cel-p (0.8μM) became weaker in the presence of competitor celastrol (1.6-6.4μM), suggesting that cel-p bond similar intracellular targets with celastrol. Cellular imaging experiments with click chemistry reaction were performed to study the cellular location of cel-p in living cells. As exhibited in Fig. 3C, cel-p mainly localized in the cell cytoplasm within 2 h and gradually entered into the cell nucleus, indicating that the cel-p was able to label cytoplasm and nuclear proteins after 4h of labeling. These data demonstrated that cel-p possessed high bioconjugation efficiency under *in situ* condition and was a suitable substitute of celastrol for subsequent chemical proteomics procedures.

Celastrol directly targeted HMBG1 and did not affect the expression of HMGB1

Next, we proceeded to identify cellular targets of celastrol by quantitative chemical proteomics technology. The protein with enrichment ratio $R_{(cel\text{-}p/cel\text{-}p+8\times cel)} > 1.5$, $p < 0.05$ was set as significant hits, and the protein information labeled by cel-p under this standard was analyzed. The identified protein hits were systematically analyzed and displayed by corresponding volcano plots after cel-p (4 μM) with or without celastrol 8 × (32 μM) treatment for 5h. A total of 1405 proteins were identified by cel-p target

recognition experiment, of which 120 were highly reliable. A complete list of identified proteins was provided in Table S1. On the basis of these criteria, HMGB1 was identified as a one of the direct binding proteins of celastrol, which has fairly high credibility and is currently one of the crucial pro-inflammatory alarmin of stroke (Fig. 4A). Primary neurons pull down, Western blot and Immunofluorescence assays verified that celastrol 8× could completely compete the binding of cel-p to HMGB1 protein, further demonstrated that HMGB1 was a direct binding protein of celastrol (Fig. 4B-D). The CETSA results also proved the direct binding of celastrol and HMGB1 protein, so as to decrease the protein degradation with increasing temperature compared with Control group (Fig. 4E-F).

As shown in Fig. 4C-D, the HMGB1 protein in celastrol 8 × (3.2 μM) group was almost invisible. In order to confirm whether high concentration of celastrol or cel-p affected the expression of HMGB1 in primary neurons, we treated normal living primary neuron with high concentration of celastrol (20 μM and 40 μM) for 5 h to evaluate its effect on HMGB1 expression with Western blot. In OGD model, we also examined the effect of cel-p (4μM) or cel-p + celastrol 8 × on HMGB1 expression in neuron cells lysate or living neuron cells. As shown in Fig. 4G, high concentration of celastrol or cel-p did not decrease the expression of HMGB1. We speculated that high concentration of celastrol occupied the binding sites of HMGB1, which led to the failure of HMGB1 protein to bind to HMGB1 antibody, rather than the degradation of HMGB1 by high concentration of celastrol or cel-p. In additon, we confirmed that celastrol had no effect on HMGB1 expression in normal cells in a certain dose and time range (Fig. 4H-K). Unexpectedly, we did not observe the time-dependent increasing secretion of HMGB1 in OGD model. On the contrary, the expression of HMGB1 in Model and M + cel groups both decreased in a time-dependent manner (Fig. 4L-N). In conclusion, celastrol directly targeted HMGB1 and did not affect the expression of HMGB1.

Celastrol played neuroprotective effect through HSP70 and NF-κB p65

As mentioned above, we did not find that celastrol affected the expression of HMGB1 in primary neurons with or without OGD insult. Celastrol induced HSP70 response and suppressed NF-κB activation to inhibit inflammatory responses and regulate innate immunity response in previous researches [28-30]. Therefore, we established OGD model *in vitro* and MCAO model *in vivo* to mimic cerebral I/R injury and tested whether celastrol affected the distribution changes of HMGB1 in the cytoplasm and nucleus and the expression changes of protein HSP70 and NF-κB p65. We found that the expression of HMGB1 in the cytoplasm of Model and M + cel group significantly increased, while the expression of HMGB1 in the nucleus obviously decreased (Fig. 5A-F).In summary, HMGB1 overall expression was barely affected by celastrol, and celastrol could hardly affect the distribution of HMGB1 in the cytoplasm and nucleus 48h after OGD injury. In contrast, celastrol significantly increased both of the overall and nucleus expression of HSP70 and decreased the overall and nucleus expression of NF-κB p65, which was consistent with previous studies [28-30] (Fig. 5A-F). The Immunofluorescence results were in line with Western blot results *in vitro* (Fig. 5J). Similar Western blot and Immunofluorescence results were also observed in MCAO rats (Fig. 5H-N). Compared with Model group, celastrol (1mg/kg) remarkable increased the expression of HSP70, down regulated the expression of NF-κB, and had no effect on the expression of HMGB1 (Fig. 5 H-N) in rats MCAO model.

Celastrol did not affect the secretion and redox state of HMGB1

HMGB1 in the concentrated supernatant of primary neuron OGD Model group increased gradually in a time-dependent manner, and reached peak at 24h (Fig. 6 A). The secreted HMGB1 in Model and M + cel (0.8 μM) group in 48h was almost the same (Fig. 6B), which indicated that celastrol did not affect the secretion of HMGB1 after OGD injury. HMGB1 in concentrated supernatant was actively secreted in response to OGD injury at 48h. Celastrol hardly affected the redox state of HMGB1, presented as the disulfide bond form HMGB1 showed a faster mobility in non-denaturing page gel and celastrol did not affect its mobility (Fig. 6C). In addition, the disulfide bond but not fully reduced form HMGB1 occupied the vast majority form of Model and M + cel group in primary neurons injured by OGD compared with Control group (Fig. 6D). According to the present results, celastrol could not affect the secretion and expression of HMGB1 protein, nor affect the redox state of HMGB1. As shown in Fig. 6E, HMGB1 includes two DNA binding domains (A, B box) and the acidic C-terminal tail. Three cysteine residues (Cys23, 45 and 106) in A, B box mainly determine the redox state of HMGB1. The disulfide bond between Cys23 and Cys45 and reduced Cys106 is indispensable for the binding of HMGB1 to TLR4 and cytokine-inducing activity [10]. Hence, we focused on whether celastrol bond with HMGB1 to weaken its cytokine activity.

Celastrol directly bond to HMGB1, HMGB1 A box and B box

Celastrol exhibited strong combining ability with recombinant human HMGB1 protein in a concentration dependent manner (Fig. 7A-B). Celastrol almost competed the binding of IAA-yne to HMGB1 or DTT reduced HMGB1 (Fig. 7C-D), which indicated that celastrol could occupy the Cys106 of disulfide HMGB1 or Cys23, 45, 106 of reduced HMGB1. This result was consistent with previous studies that celastrol was proposed to exert cellular effects by forming covalent adducts with cysteine residues of proteins [31-33]. The binding ability of celastrol to HMGB1 protein was stronger than GA and Metformin, which were recognized HMGB1 inhibitors by binding to A, B box and C-terminal acidic tail of HMGB1 respectively (Fig. 7E-F). Celastrol also almost completely blocked the binding of IAA-yne to cysteines group of recombinant human HMGB1 A, B box. The binding of cel-p to A and B box could not be blocked by IAA (Fig. 7 G), which indicated that celastrol could bind to other sites of HMGB1 in addition to the cysteines 23, 45 and 106.

Celastrol remarkably blocked the cytokine activity of HMGB1 and B box

Celastrol did not affect the expression and redox state of HMGB1 after OGD injury. In addition, previous research indicated that only disulfide bond form HMGB1 possessed cytokine activity[10]. Therefore, we mainly explored whether celastrol influenced the disulfide bond form HMGB1 induced TNF-α increase in RAW 264.7 cells. According to the description of the manual, EC_{50} of HMGB1 for stimulating RAW 264.7 cells TNF-α production was 0.7855-0.8342μg/ml, so we chose 0.8 μg/ml HMGB1 to induce the secretion of TNF-α. As shown in Fig. 8A, 0.8μg/ml HMGB1 obviously increased the TNF-α secretion compared with control group, and 0.1μM or 0.05μM celastrol apparently decreased the TNF-α secretion in RAW 264.7 cells. 0.02μg/ml and 0.2μg/ml recombinant human HMGB1 B box obviously increased the TNF-α secretion compared with control group, and 1× (10^{-6}μmol and 10^{-5}μmol) celastrol apparently decreased

the TNF-α secretion in RAW 264.7 cells (Fig. 8B). According to the published literature, TLR4 is the only receptor of HMGB1 for producing cytokine by binding to the B box cysteine 106 [34]. Then we utilized recombinant human B box, B box-celastrol complex to verify that 1× and 5× celastrol obviously blocked the binding of receptors TLR4 and RAGE to B box (Fig. 8C). In conclusion, celastrol remarkably blocked the cytokine activity of HMGB1 and B box by directly binding to them to block the combination of inflammatory receptors with them.

Discussions

Our studies demonstrated that: (1) celastrol exhibited neuroprotective effect for ischemic stroke *in vitro* and *in vivo*; (2) celastrol directly bond the HMGB1; (3) celastrol did not affect the expression of HMGB1, increased the HSP70 and decreased the NF-κB expression to play anti-inflammatory effect *in vitro* and *in vivo*; (4) celastrol bond the 106 cysteine of disulfide bond HMGB1 or 23, 45, 106 cysteines of fully reduced HMGB1; (5) celastrol scavenged the overproduced TNF-α induced by disulfide bond HMGB1 and B box; and (6) celastrol played anti-inflammatory effect by binding to the B box to block the combination of TLR4 and RAGE with HMGB1 B box . Taken together, our findings suggested that the neuroprotective action of celastrol for ischemic stroke was due to its inhibition of neuroinflammation effect through up regulating HSP70 and decreasing NF-κB expression and directly binding with HMGB1 protein. The specific experimental process was shown in Fig. 9.

With the maturation of Mass-spectrometry based proteomics technology, stable isotopes label has been widely used in the research of biomarkers for diseases and drugs targets through quantitative measurement of relative or absolute protein amounts in healthy versus disease states [35]. TMT and iTRAQ are commercially available and widespread application isobaric tag for they allow multiplexing of up to 10 samples with high-resolution instruments and a range of sample types applicable [36]. TMT isobaric labeling could simultaneous identification and quantification of the complex protein mixtures components with the key workflow of sample denaturation, digestion, isobaric tagging of tryptic peptides, fractionation, mass spectrometric analysis and data processing [37, 38]. First, we verified that celastrol remained biological activity after introducing biorthogonal reaction groups. Celastrol exhibited neuroprotective effect for ischemic stroke *in vitro* and *in vivo*. With the aiding of cel-p, TMT label and LC-MS/MS technologies, we identified 1405 proteins in cel-p target recognition experiment, of which 120 were highly reliable. HMGB1 was identified as a direct binding protein of celastrol with fairly high credibility (Fig. 4).

CETSA is a label-free biophysical technique for studies of target engagement in cells and tissues based on ligand binding affects protein stability and cellular studies of proteins redox modulations [39]. Generally speaking, many proteins unfold after heating and precipitate rapidly in cells, and drug binding protein can stabilize the protein and reduce its degradation with increasing temperature compared with no treated cells [40]. CETSA based on immunoassays (such as Western blot, proximity ligation assays, mass spectrometry) detection is a hot technique to validate ligand binding of drugs to proteins in lysates, cells and tissues, which is based on measuring the protein melting curves changes after different heating

steps and quantifying the amount of remaining soluble protein [40, 41]. We investigated whether celastrol combined with HMGB1 and stabilized HMGB1 in cell lysate samples subjected to temperatures from 37 to 82 °C. The results showed that compared with DMSO treated control group, the celastrol treated group significantly stabilized the HMGB1 and decreased its degradation with temperature increase (Fig. 4E-F).

HMGB1 is highly expressed in the nucleus of multiple cell types, and the redox state of intracellular and extracellular HMGB1 is dynamic mainly related with the 23, 45, and 106 cysteines. Disulfide bond form of HMGB1 (C106 in thiol and C23, C45 form disulfide bond) is requisite for TLR4/MD-2 interaction to induce TNF release and NF-κB activation [10]. HMGB1 can be released by passive or active secretion via multiple pathways. Passive release of HMGB1 occurs rapidly during primary necrosis with fully reduced or disulfide forms, or nuclear retention and passive release during cell apoptosis secondary necrosis with mainly fully oxidized form (sulfonyl HMGB1). Active secretion happen late stage in pyroptosis with post-translational modification and mainly disulfide form [12]. Previous studies showed that celastrol significantly suppressed HMGB1/NF-κB pathway to alleviate inflammatory pain and exhibit neuroprotective effect in transient global cerebral I/R, and inhibited HMGB1 expression to decrease myocardial I/R injury [8, 42, 43]. Different from previous studies, the peak expression of HMGB1 was not detected in the Model group, and celastrol did not affect the expression of HMGB1. The results of this experiment may be related to the type of cells we selected. Because mammalian neurons are terminally differentiated, postmitotic cells, and the isolated rat cortex primary neurons have little ability of division and proliferation *in vitro* in the absence of inducer [44]. The neuron cell culture medium supernatant Western blot results proved that primary neurons suffering from OGD injury mainly actively secreted disulfide bond form of HMGB1, and the formation of disulfide bond could hardly be prevented by celastrol (Fig. 6). Plasma HMGB1 rapidly increases and acts as a pro-inflammatory cytokine to activate microglia, aggravate excite-toxicity induced neuronal death and aggravate brain injury during the acute damaging phase of ischemic insult [45, 46]. Early HMGB1 translocation and release occurs mostly in injured neurons and acts as a proinflammatory cytokine by interacting with receptors of RAGE, TLR2 and TLR4 [47]. High levels of HMGB1 in the serum and cerebrospinal fluid (CSF) are related with severity of animal ischemic brain damage. In addition, HMGB1 in the serum of lipopolysaccharide (LPS) administered MCAO animals was up-regulated and mainly disulfide bond type [48]. Blockade of HMGB1 with antagonists has been verified an effective treating style for animal stroke model, including GA [49], HMGB1 A box, anti-HMGB1 monoclonal antibody [50]. Previous studies demonstrated that peripheral disulfide HMGB1 produced more obvious pro-nociceptive activity than all-thiol HMGB1 via activating TLR4 other than RAGE [51]. Here, we confirmed that celastrol did not affect the secretion, redox state and expression of HMGB1 both in normal and OGD insult neuron cells. Apart from binding with the cysteines, celastrol also occupied other sites of HMGB1. Considering that only disulfide bond form HMGB1 has cytokine property, we focused on the effect of celastrol on disulfide bond form HMGB1. 106 cysteine is the main binding site of TLR4 receptor to HMGB1 to play cytokine activity. In our research, celastrol directly bond to HMGB1 A, B box and blocked the binding of HMGB1 B box to its receptors TLR4 and RAGE, resulting in inflammatory activity loss. Celastrol disrupted the TNF-α inducing capacity of HMGB1 and B box in RAW264.7 cells. Therefore, celastrol directly bond to HMGB1 to make it lose inflammatory

activity, rather than reducing its secretion or changing its redox activity. In addition, celastrol played anti-inflammatory effect in cerebral ischemic injury by targeting HSP70 and NF-κB.

Although celastrol and its numerous derivatives exhibit potential therapeutic effects against various diseases, none of them have been approved for clinical use due to their toxic effects, low solubility and narrow therapeutic dose range [52]. Therefore, how to solve the toxicity of celastrol and improve its efficacy is the next focus direction. In addition, a growing body of evidence supports the idea that inflammation plays different roles in different stages of stroke [53]. HMGB1 shows different activities according to redox modifications, and may play a more complex role in ischemic stroke to be explored. In addition to cytokine activity, HMGB1 also exerts beneficial effects in axonal regeneration, endothelial activation, angiogenesis, neurovascular repair and remodeling [11, 54]. Therefore, it is necessary to consider carefully about promoting or inhibiting HMGB1 in different stages of stroke.

Conclusion

In summary, we performed a proteome-wide investigation of direct cellular protein binding targets of celastrol in primary neuron, and identified 120 targets with fairly high credibility through quantitative chemical proteomics approach. The present study demonstrated the neuroprotective effect of celastrol against cerebral I/R injury through targeting HSP70 and NF-κB and disrupting the cytokine activity of disulfide bond HMGB1 in rat primary cortical neurons OGD model and adult rats MCAO model, which may provide a potential therapeutic direction for ischemic stroke therapy. By directly binding to the B box, celastrol blocked the binding of TLR4 and RAGE receptors with B box to exhibit anti-inflammatory activity. To the best of our knowledge, this is the first study to evaluate the direct binding of celastrol to protein HMGB1. We hope that the data and findings from the present study can provide useful guidance for the clinical use of celastrol in future.

Abbreviations

OGD: oxygen-glucose deprivation; MCAO: middle cerebral artery occlusion; TMT: tandem mass tags; CETSA: cellular thermal shift assay; HMGB1: high mobility group protein 1; DAMP: damage-associated molecular pattern; RAGE: Receptor for advanced glycation end products; TLR: toll like receptor; TNF: tumor necrosis factor ; cel-p: celastrol probe; LC-MS/MS: liquid chromatography-tandem mass spectrometry; DMEM: Dulbecco's modified Eagle medium; FBS: fetal bovine serum; DMSO: dimethylsulfoxide; I/R: ischemic-reperfusion; SDS-PAGE: sodium dodecyl sulfate-polyacrylamide gel electrophoresis; LPS: lipopolysaccharide;CBB: Coomassie brilliant blue; GA: Glycyrrhetinic acid; Mel: Melatonin; TTC: 2, 3, 5-triphenyltetrazolium chloride; DTT: Dithiothreitol; CSF: cerebrospinal fluid; IPTG: Isopropyl-D-1-thiogalactopyranoside.

Declarations

Authors' contributions

JW and NM designed the experiments; DL and PL performed the experiments; QZ, PG, YZ and JZ assisted with experiments; NM analyzed the data and contributed analysis tools; DL wrote the manuscript; LG and XC revised the manuscript. The authors read and approved the final manuscript.

Funding

We gratefully acknowledge financial support from the National Natural Science Foundation of China (81903588, 81803456, 81702580 and 81841001), TCM One Belt and One Road Project of CACMS (GH201807), the Major National Science and Technology Program of China for Innovative Drug (2017ZX09101002-001-001-05), and the Fundamental Research Funds for the Central Public Welfare Research Institutes (ZXKT18003).

Availability of data and materials

The datasets and materials supporting the conclusions of this article are included within the article.

Ethics approval and consent to participate

All experiments animal operations meet the requirements of the Beijing Administration Rule of Laboratory Animal, and were approved by the Animal Experimental Ethics Review Committee of the Institute of Basic Research for Chinese Medicine, China Academy of Chinese Medical Sciences.

Consent for publication

Not applicable.

Conflict of interest

The authors declare that there are no conflicts of interest.

References

1. Zhang Y, Mao X, Li W, Chen W, Wang X, Ma Z, Lin N. **Tripterygium wilfordii: An inspiring resource for rheumatoid arthritis treatment**. *Medicinal research reviews* 2020.
2. Yizhi C, Zhixiang, Gong, Xiangmei, Chen, Li. Tang, Xuezhi, Zhao: **Tripterygium wilfordii Hook F (a traditional Chinese medicine) for primary nephrotic syndrome**. *Cochrane Database of Systematic Reviews* 2013.
3. Lu Y, Liu Y, Zhou J, Li D, Gao W. **Biosynthesis, total synthesis, structural modifications, bioactivity, and mechanism of action of the quinone-methide triterpenoid celastrol**. *Medicinal research reviews* 2020.
4. Xu S, Feng Y, He W, Xu W, Xu W, Yang H, Li X. **Celastrol in Metabolic Diseases: Progress and Application Prospects**. *Pharmacological research* 2021:105572.

5. Li J, Hao J. Tripterygium wilfordiiTreatment of Neurodegenerative Diseases with Bioactive Components of. Am J Chin Med. 2019;47:769–85.
6. Jiang M, Liu X, Zhang D, Wang Y, Hu X, Xu F, Jin M, Cao F, Xu L. Celastrol treatment protects against acute ischemic stroke-induced brain injury by promoting an IL-33/ST2 axis-mediated microglia/macrophage M2 polarization. J Neuroinflamm. 2018;15:78.
7. Li Y, He D, Zhang X, Liu Z, Zhang X, Dong L, Xing Y, Wang C, Qiao H, Zhu C, Chen Y. Protective effect of celastrol in rat cerebral ischemia model: down-regulating p-JNK, p-c-Jun and NF-κB. Brain research. 2012;1464:8–13.
8. Zhang B, Zhong Q, Chen X, Wu X, Sha R, Song G, Zhang C, Chen X. Neuroprotective Effects of Celastrol on Transient Global Cerebral Ischemia Rats via Regulating HMGB1/NF-κB Signaling Pathway. Front NeuroSci. 2020;14:847.
9. Maida C, Norrito R, Daidone M, Tuttolomondo A, Pinto A. **Neuroinflammatory Mechanisms in Ischemic Stroke: Focus on Cardioembolic Stroke, Background, and Therapeutic Approaches**. *International journal of molecular sciences* 2020, 21.
10. Yang H, Antoine D, Andersson U, Tracey K. The many faces of HMGB1: molecular structure-functional activity in inflammation, apoptosis, and chemotaxis. J Leukoc Biol. 2013;93:865–73.
11. Singh V, Roth S, Veltkamp R, Liesz A. HMGB1 as a Key Mediator of Immune Mechanisms in Ischemic Stroke. Antioxid Redox Signal. 2016;24:635–51.
12. Harris H, Andersson U, Pisetsky D. HMGB1: a multifunctional alarmin driving autoimmune and inflammatory disease. Nature reviews Rheumatology. 2012;8:195–202.
13. Venereau E, Casalgrandi M, Schiraldi M, Antoine D, Cattaneo A, De Marchis F, Liu J, Antonelli A, Preti A, Raeli L, et al. Mutually exclusive redox forms of HMGB1 promote cell recruitment or proinflammatory cytokine release. The Journal of experimental medicine. 2012;209:1519–28.
14. Yang H, Wang H, Ju Z, Ragab A, Lundbäck P, Long W, Valdes-Ferrer S, He M, Pribis J, Li J, et al. MD-2 is required for disulfide HMGB1-dependent TLR4 signaling. The Journal of experimental medicine. 2015;212:5–14.
15. Wang J, Gao L, Lee Y, Kalesh K, Ong Y, Lim J, Jee J, Sun H, Lee S, Hua Z, Lin Q. Target identification of natural and traditional medicines with quantitative chemical proteomics approaches. Pharmacol Ther. 2016;162:10–22.
16. Wang J, Zhang C, Chia W, Loh C, Li Z, Lee Y, He Y, Yuan L, Lim T, Liu M, et al. Haem-activated promiscuous targeting of artemisinin in Plasmodium falciparum. Nature communications. 2015;6:10111.
17. Wang J, Tan X, Nguyen V, Yang P, Zhou J, Gao M, Li Z, Lim T, He Y, Ong C, et al. A quantitative chemical proteomics approach to profile the specific cellular targets of andrographolide, a promising anticancer agent that suppresses tumor metastasis. Molecular cellular proteomics: MCP. 2014;13:876–86.
18. Wang J, Zhang J, Zhang C, Wong Y, Lim T, Hua Z, Liu B, Tannenbaum S, Shen H, Lin Q. In situ Proteomic Profiling of Curcumin Targets in HCT116 Colon Cancer Cell Line. Scientific reports.

2016;6:22146.

19. Wang J, Zhang C, Zhang J, He Y, Lee Y, Chen S, Lim T, Ng S, Shen H, Lin Q. Mapping sites of aspirin-induced acetylations in live cells by quantitative acid-cleavable activity-based protein profiling (QA-ABPP). Scientific reports. 2015;5:7896.
20. Chen T, Chen S, Wang D, Hung H. The Cholinergic Signaling Responsible for the Expression of a Memory-Related Protein in Primary Rat Cortical Neurons. Journal of cellular physiology. 2016;231:2428–38.
21. Yu Z, Liu N, Li Y, Xu J, Wang X. Neuroglobin overexpression inhibits oxygen-glucose deprivation-induced mitochondrial permeability transition pore opening in primary cultured mouse cortical neurons. Neurobiol Dis. 2013;56:95–103.
22. Cheng K, Lee J, Hao P, Yao S, Ding K, Li Z. Tetrazole-Based Probes for Integrated Phenotypic Screening, Affinity-Based Proteome Profiling, and Sensitive Detection of a Cancer Biomarker. Angew Chem. 2017;56:15044–8.
23. Ma N, Hu J, Zhang Z, Liu W, Huang M, Fan Y, Yin X, Wang J, Ding K, Ye W, Li Z. H2-Azirine-Based Reagents for Chemoselective Bioconjugation at Carboxyl Residues Inside Live Cells. J Am Chem Soc. 2020;142:6051–9.
24. Liu DD, Zou C, Zhang J, Gao P, Wang J. *Target Profiling of an Anticancer Drug by an In Situ Approach*. 2021.
25. Hengst J, Dick T, Smith C, Yun J. Analysis of selective target engagement by small-molecule sphingosine kinase inhibitors using the Cellular Thermal Shift Assay (CETSA). Cancer Biol Ther. 2020;21:841–52.
26. Kobayashi Y, Kanesaki Y, Tanaka A, Kuroiwa H, Kuroiwa T, Tanaka K. Tetrapyrrole signal as a cell-cycle coordinator from organelle to nuclear DNA replication in plant cells. Proc Natl Acad Sci USA. 2009;106:803–7.
27. Zhang Z, Liu D, Jiang J, Song X, Zou X, Chu S, Xie K, Dai J, Chen N, Sheng L, Li Y. Metabolism of IMM-H004 and Its Pharmacokinetic-Pharmacodynamic Analysis in Cerebral Ischemia/Reperfusion Injured Rats. Front Pharmacol. 2019;10:631.
28. Salminen A, Lehtonen M, Paimela T, Kaarniranta K. Celastrol: Molecular targets of Thunder God Vine. Biochem Biophys Res Commun. 2010;394:439–42.
29. Zhao Y, Zhao H, Lobo N, Guo X, Gentleman S, Ma D. Celastrol enhances cell viability and inhibits amyloid-β production induced by lipopolysaccharide in vitro. Journal of Alzheimer's disease: JAD. 2014;41:835–44.
30. Paimela T, Hyttinen J, Viiri J, Ryhänen T, Karjalainen R, Salminen A, Kaarniranta K. Celastrol regulates innate immunity response via NF-κB and Hsp70 in human retinal pigment epithelial cells. Pharmacological research. 2011;64:501–8.
31. Boridy S, Le P, Petrecca K, Maysinger D. Celastrol targets proteostasis and acts synergistically with a heat-shock protein 90 inhibitor to kill human glioblastoma cells. Cell death disease. 2014;5:e1216.

32. Klaić L, Morimoto R, Silverman R. Celastrol analogues as inducers of the heat shock response. Design and synthesis of affinity probes for the identification of protein targets. ACS chemical biology. 2012;7:928–37.
33. Zhang D, Chen Z, Hu C, Yan S, Li Z, Lian B, Xu Y, Ding R, Zeng Z, Zhang X, Su Y. Celastrol binds to its target protein via specific noncovalent interactions and reversible covalent bonds. Chem Commun (Cambridge England). 2018;54:12871–4.
34. Yang H, Hreggvidsdottir H, Palmblad K, Wang H, Ochani M, Li J, Lu B, Chavan S, Rosas-Ballina M, Al-Abed Y, et al. A critical cysteine is required for HMGB1 binding to Toll-like receptor 4 and activation of macrophage cytokine release. Proc Natl Acad Sci USA. 2010;107:11942–7.
35. Chahrour O, Cobice D, Malone J. Stable isotope labelling methods in mass spectrometry-based quantitative proteomics. J Pharm Biomed Anal. 2015;113:2–20.
36. Ankney J, Muneer A, Chen X. Relative and Absolute Quantitation in Mass Spectrometry-Based Proteomics. Annual review of analytical chemistry (Palo Alto Calif). 2018;11:49–77.
37. Westbrook J, Noirel J, Brown J, Wright P, Evans C. Quantitation with chemical tagging reagents in biomarker studies. Proteomics Clinical applications. 2015;9:295–300.
38. Thompson A, Schäfer J, Kuhn K, Kienle S, Schwarz J, Schmidt G, Neumann T, Johnstone R, Mohammed A, Hamon C. Tandem mass tags: a novel quantification strategy for comparative analysis of complex protein mixtures by MS/MS. Analytical chemistry. 2003;75:1895–904.
39. Sun W, Dai L, Yu H, Puspita B, Zhao T, Li F, Tan J, Lim Y, Chen M, Sobota R, et al. Monitoring structural modulation of redox-sensitive proteins in cells with MS-CETSA. Redox Biol. 2019;24:101168.
40. Martinez Molina D, Nordlund P. The Cellular Thermal Shift Assay: A Novel Biophysical Assay for In Situ Drug Target Engagement and Mechanistic Biomarker Studies. Annu Rev Pharmacol Toxicol. 2016;56:141–61.
41. Dai L, Prabhu N, Yu L, Bacanu S, Ramos A, Nordlund P. Horizontal Cell Biology: Monitoring Global Changes of Protein Interaction States with the Proteome-Wide Cellular Thermal Shift Assay (CETSA). Annual review of biochemistry. 2019;88:383–408.
42. Zhang X, Zhao W, Liu X, Huang Z, Shan R, Huang C. Celastrol ameliorates inflammatory pain and modulates HMGB1/NF-κB signaling pathway in dorsal root ganglion. Neurosci Lett. 2019;692:83–9.
43. Tong S, Zhang L, Joseph J, Jiang X. **Celastrol pretreatment attenuates rat myocardial ischemia/reperfusion injury by inhibiting high mobility group box 1 protein expression via the PI3K/Akt pathway.** *Biochemical and biophysical research communications* 2018, 497:843–849.
44. Aranda-Anzaldo A, Dent M. Why Cortical Neurons Cannot Divide, and Why Do They Usually Die in the Attempt? J Neurosci Res. 2017;95:921–9.
45. Kim J, Sig Choi J, Yu Y, Nam K, Piao C, Kim S, Lee M, Han P, Park J, Lee J. HMGB1, a novel cytokine-like mediator linking acute neuronal death and delayed neuroinflammation in the postischemic brain. The Journal of neuroscience: the official journal of the Society for Neuroscience. 2006;26:6413–21.

46. Kim S, Lim C, Kim J, Shin J, Lee S, Lee M, Lee J. Extracellular HMGB1 released by NMDA treatment confers neuronal apoptosis via RAGE-p38 MAPK/ERK signaling pathway. Neurotox Res. 2011;20:159–69.
47. Qiu J, Nishimura M, Wang Y, Sims J, Qiu S, Savitz S, Salomone S, Moskowitz M. Early release of HMGB-1 from neurons after the onset of brain ischemia. Journal of cerebral blood flow metabolism: official journal of the International Society of Cerebral Blood Flow Metabolism. 2008;28:927–38.
48. Kim I, Lee H, Kim S, Lee H, Choi J, Han P, Lee J. Alarmin HMGB1 induces systemic and brain inflammatory exacerbation in post-stroke infection rat model. Cell death disease. 2018;9:426.
49. Kim S, Jin Y, Shin J, Kim I, Lee H, Park S, Han P, Lee J. Glycyrrhizic acid affords robust neuroprotection in the postischemic brain via anti-inflammatory effect by inhibiting HMGB1 phosphorylation and secretion. Neurobiol Dis. 2012;46:147–56.
50. Nishibori M, Mori S, Takahashi H. Anti-HMGB1 monoclonal antibody therapy for a wide range of CNS and PNS diseases. J Pharmacol Sci. 2019;140:94–101.
51. Yamasoba D, Tsubota M, Domoto R, Sekiguchi F, Nishikawa H, Liu K, Nishibori M, Ishikura H, Yamamoto T, Taga A, Kawabata A. Peripheral HMGB1-induced hyperalgesia in mice: Redox state-dependent distinct roles of RAGE and TLR4. J Pharmacol Sci. 2016;130:139–42.
52. Hou W, Liu B, Xu H. Celastrol: Progresses in structure-modifications, structure-activity relationships, pharmacology and toxicology. Eur J Med Chem. 2020;189:112081.
53. Jayaraj R, Azimullah S, Beiram R, Jalal F, Rosenberg G. Neuroinflammation: friend and foe for ischemic stroke. J Neuroinflamm. 2019;16:142.
54. Richard S, Sackey M, Su Z, Xu H. **Pivotal neuroinflammatory and therapeutic role of high mobility group box 1 in ischemic stroke**. *Bioscience reports* 2017, 37.

Tables

Table 1 Primary antibodies

Primary antibodies	Host	Dilution ratio	Supplier
MAP2	Mouse	1:500 (IF)	Abcam, United States
β-tubulin	Rabbit	1:500 (IF)	Abcam, United States
β-actin	Mouse	1:5000 (WB)	Affinity Biosciences, USA
PCNA	Rabbit	1:3000 (WB)	Proteintech Group, USA
NF-κB p65	Mouse	1:1000 (WB)	Proteintech Group, USA
		1:500 (IF)	
HSP70	Rabbit	1:1000 (WB)	Abcam, United States
		1:500 (IF)	
HMGB1	Rabbit	1:1000 (WB)	Abcam, United States
		1:500 (IF)	
RAGE	Rabbit	1:1000 (WB)	Proteintech Group, USA
TLR4	Rabbit	1:1000 (WB)	Proteintech Group, USA

Figures

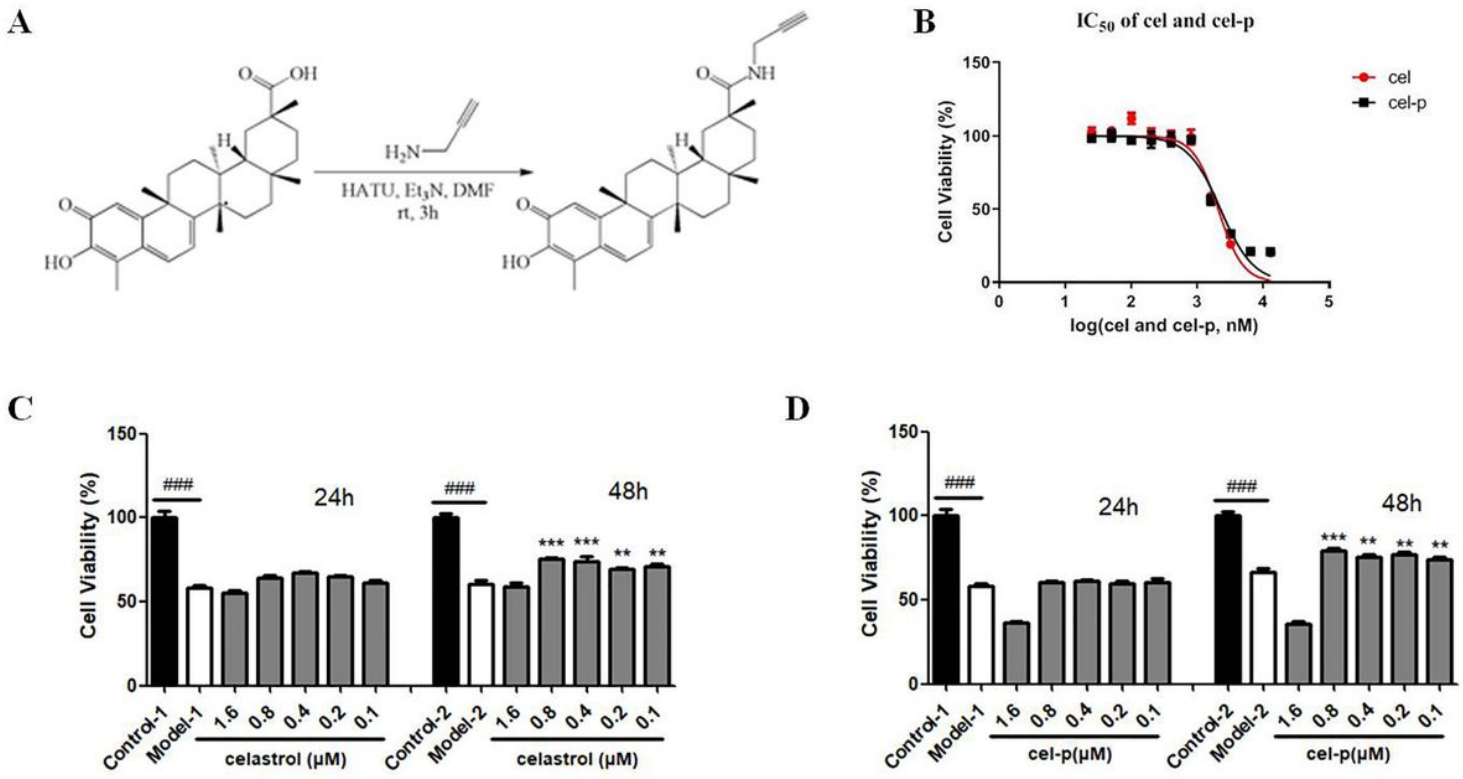

Figure 1

(A) Chemical structure and specific synthesis route of cel-p. (B) Dose-response curves of celastrol and cel-p in living primary neurons suggested that cel-p closely mimicked the original compound in biological activity (celastrol IC50 = 2.2 μM, cel-p IC50 = 2.0 μM). (C-D) Celastrol and cel-p showed similar neuroprotective effect on OGD model of primary neurons in vitro. The optimal dose of celastrol and cel-p was 0.1-0.8 μM, and the optimal administration time was 48 h after OGD model. Error bars represent SEM. ###p<0.001 vs. Control group, *p<0.05, **p<0.01, ***p<0.001 vs. Model group, One-way analysis of variance was used (n=6).

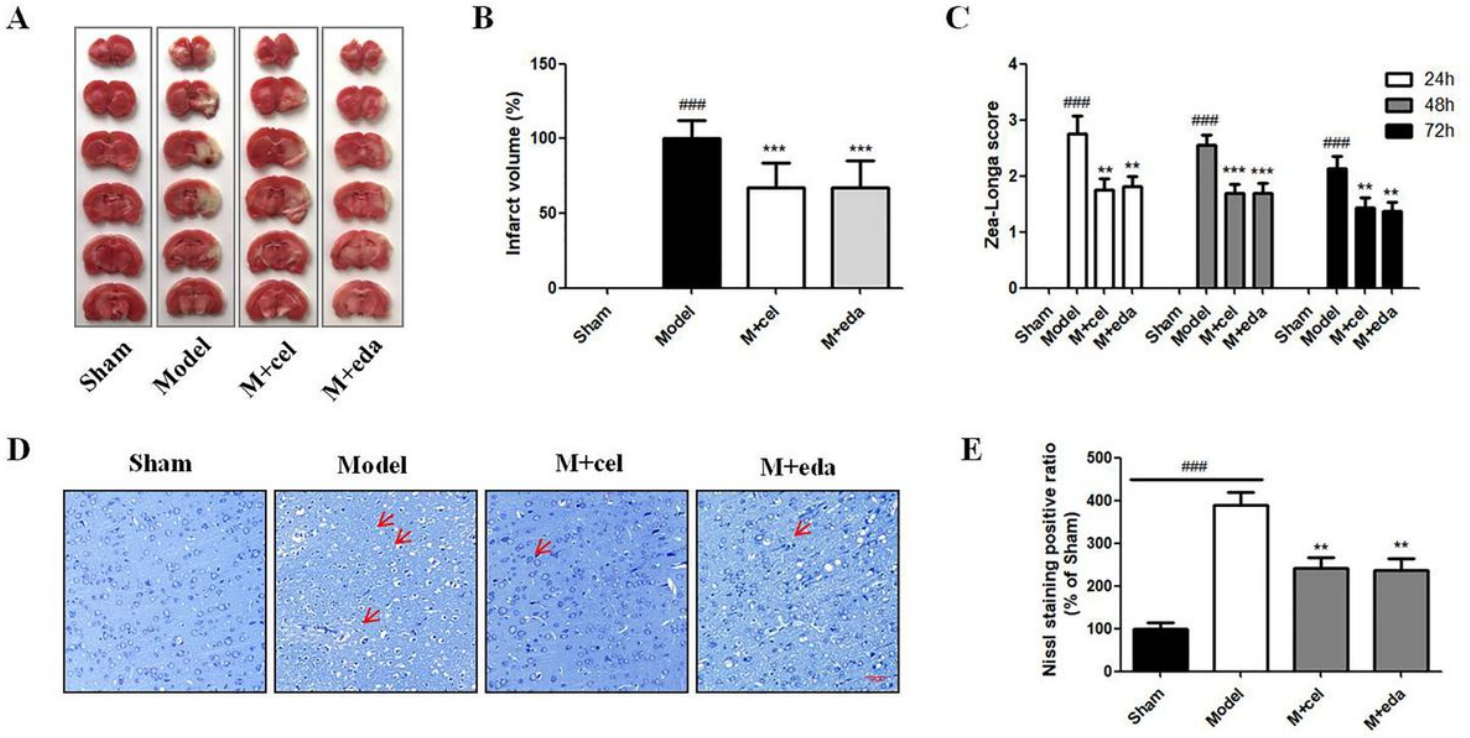

Figure 2

Celastrol (1mg/kg, i.p.) significantly reduced the volume of cerebral infarction, improved behavior indexes and Nissl staining scores of MCAO rats. (A) Representative brain slices stained by TTC. (B) Quantitative evaluation of infarct volume. (C) The results of Zea-Longa score indicated that celastrol (1mg/kg, i.p.) and edaravone injection (6mg/kg, i.v.) improved behavior indexes of MCAO rats at 24 h, 48 h and 72 h. (D, E) Compared with Sham group, extensive neuronal cells loss, nuclear shrinkage, and dark staining were visualized in the cortex of Model group. Administration of celastrol or edaravone markedly reduced these pathological changes. Error bars represent SEM. ###p<0.001 vs. Sham group, *p<0.05, **p<0.01, ***p<0.001 vs. Model group, One-way analysis of variance was used (n=8, Nissl staining n=3). Scale bar = 200 μm.

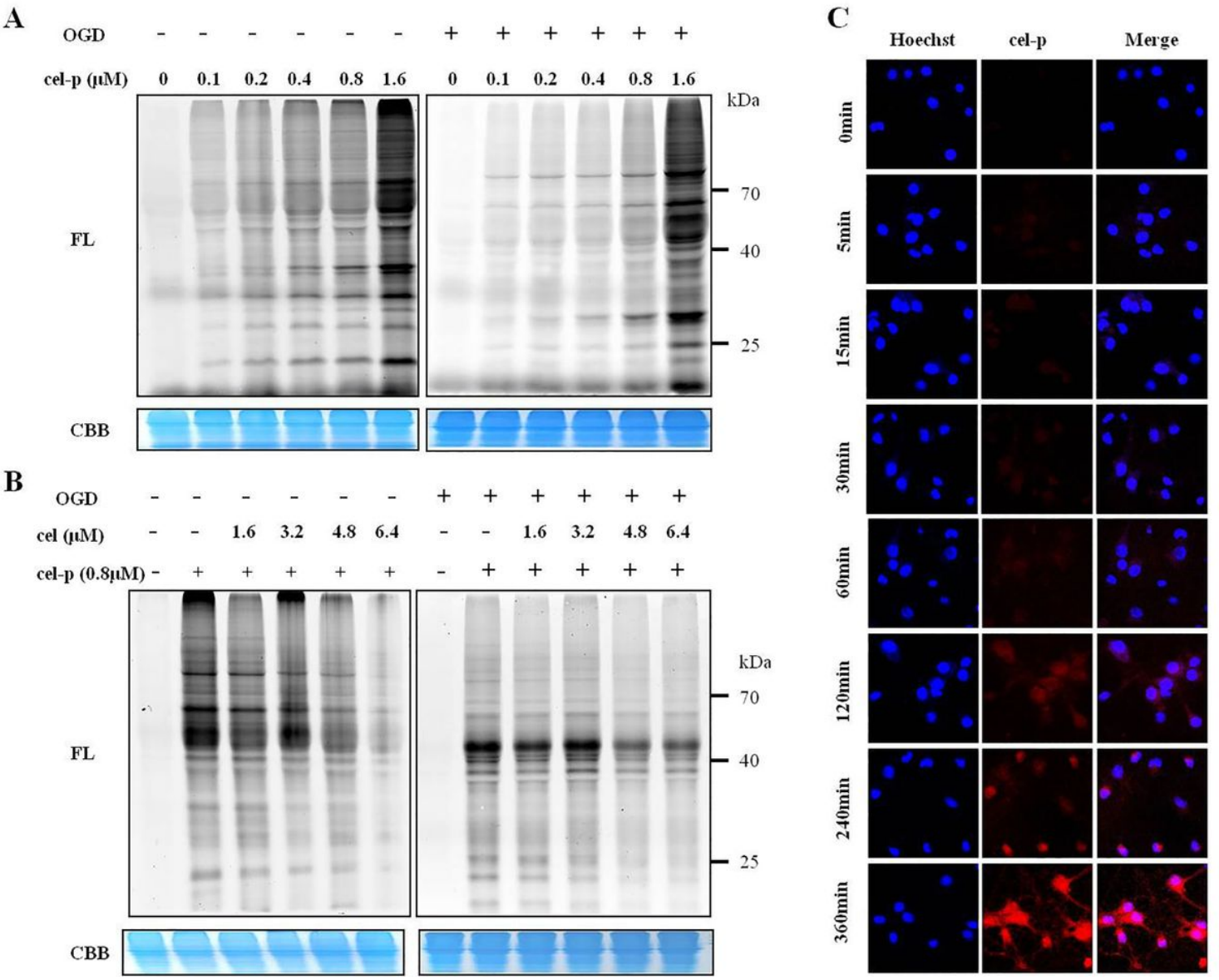

Figure 3

Labeling profiles of cel-p in living primary neurons. (A) Concentration-dependent (0-1.6 μM) labeling profiles of cel-p in normal and OGD injury primary neurons. (B) Competitive labeling profiles of cel-p (0.8 μM) in normal and OGD injury primary neurons in the presence of celastrol (2 ×, 4 ×, 6 ×, 8 ×). (C) Cel-p mainly localized in the cell cytoplasm within 2 h and gradually entered into the cell nucleus after 2 h. FL = in-gel fluorescence scanning, CBB = Coomassie brilliant blue gel.

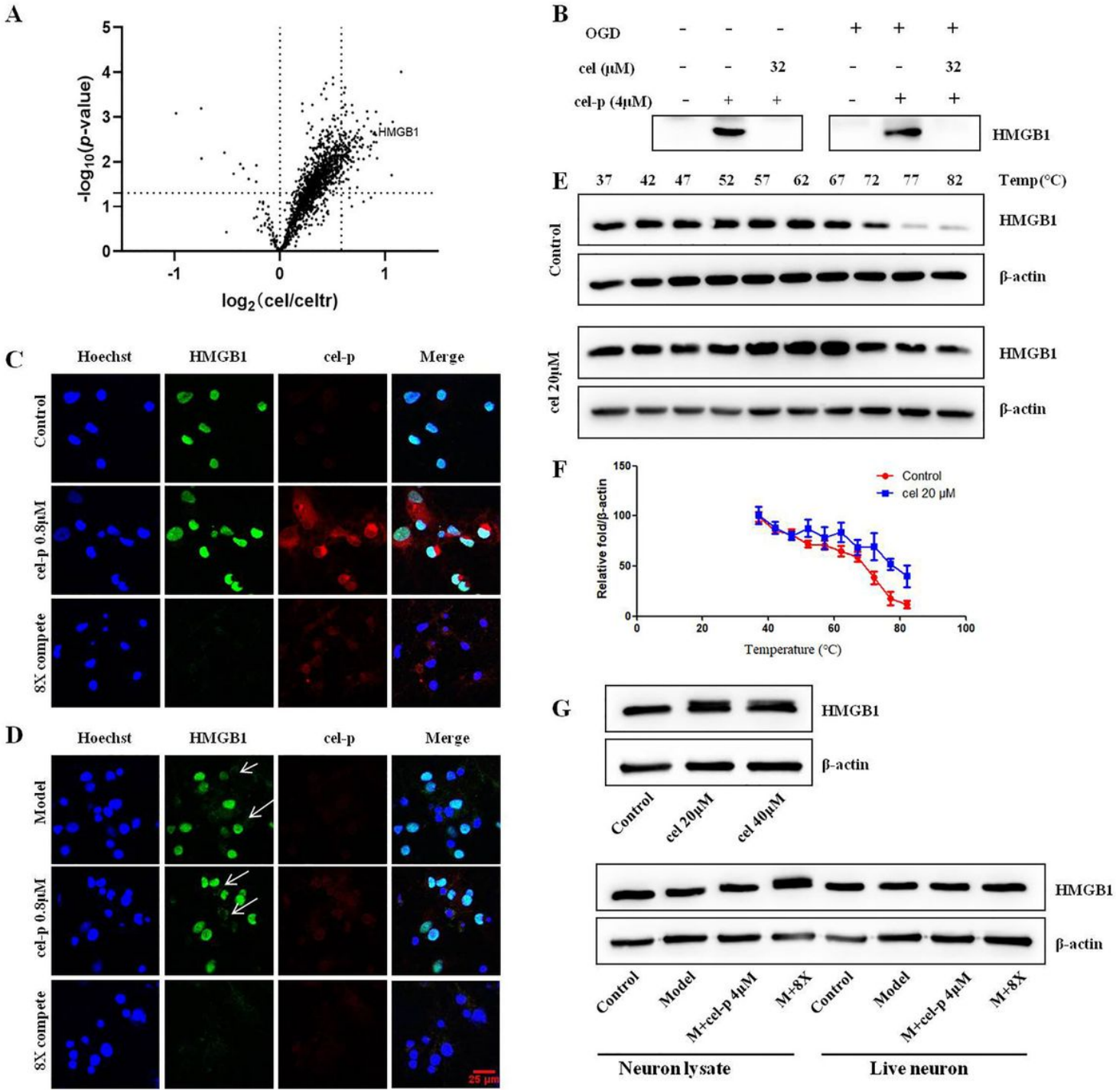

Figure 4

(A) Quantitative mass spectrometry-based profiling of cel-p (4 μM) in the presence of celastrol 8×, and HMGB1 protein had a high degree of credibility. (B-D) Target validation of HMGB1 by pull-down, Western blot and Immunofluorescence assays in living primary neurons under normal or OGD condition verified that celastrol 8× could completely compete the binding of cel-p to HMGB1 protein. (E, F) The CETSA results proved that celastrol directly bond with HMGB1 protein to decrease the protein degradation with increasing temperature. (G) High concentration of celastrol or cel-p did not affect the expression of HMGB1 in neurons within 5h. (H-K) Celastrol had no effect on HMGB1 expression in normal primary

neuron within 48 h and 0.1-0.8μM. (L-N) The content of HMGB1 in Model and M + cel groups both decreased with time.

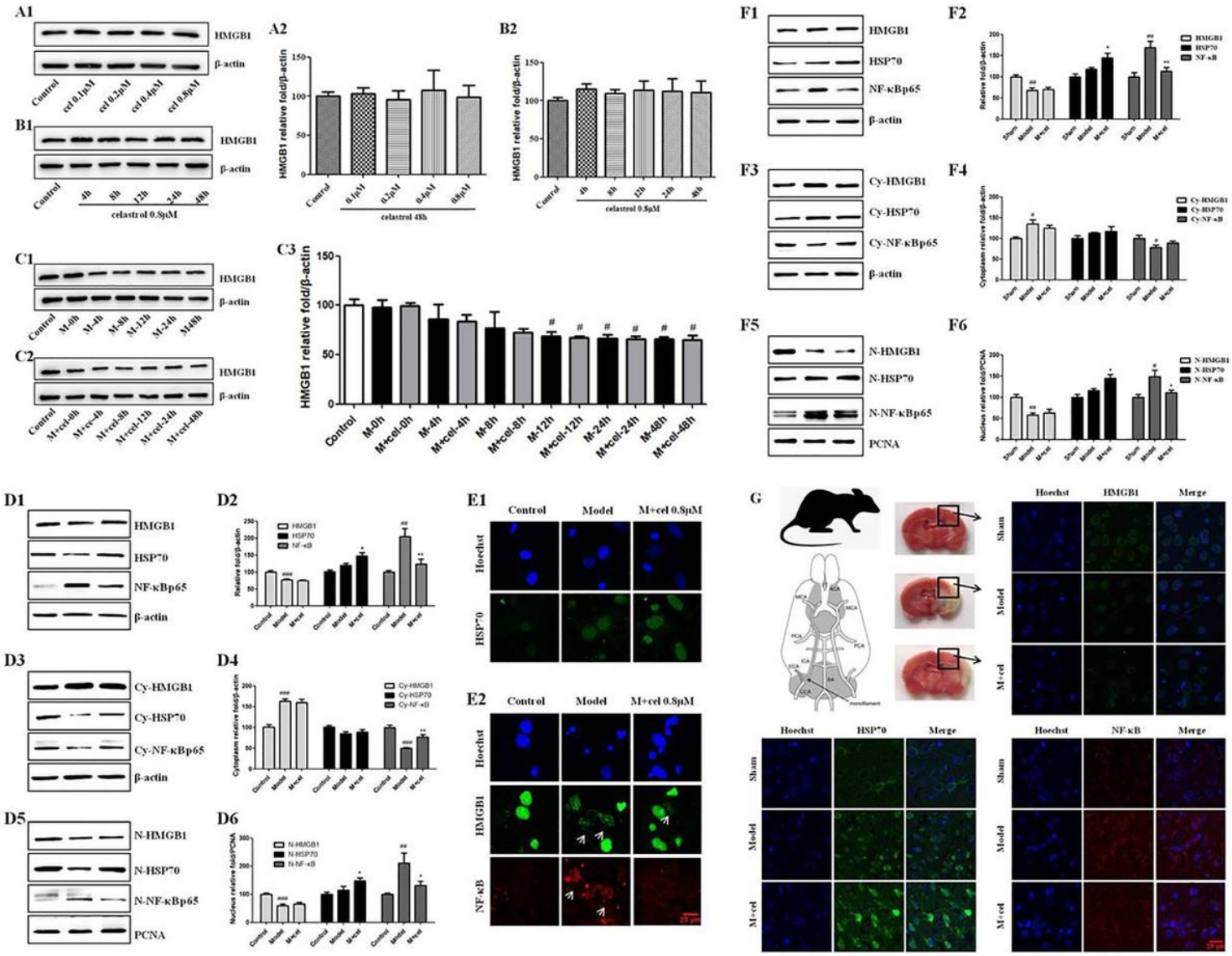

Figure 5

(A-J) The changes of HMGB1, HSP70 and NF-κB protein affected by OGD model and celastrol were observed at 48 h with Western blot and Immunofluorescence in vitro. (H-N) The changes of HMGB1, HSP70 and NF-κB protein were observed at rat cerebral cortex with Western blot and rat cerebral cortex slices with Immunofluorescence. Error bars represent SEM. ###p<0.001 vs. Control group (in vitro) or Sham group (in vivo), *p<0.05, **p□0.01, ***p<0.001 vs. Model group, One-way analysis of variance was used (n=4). Scale bar=25μm.

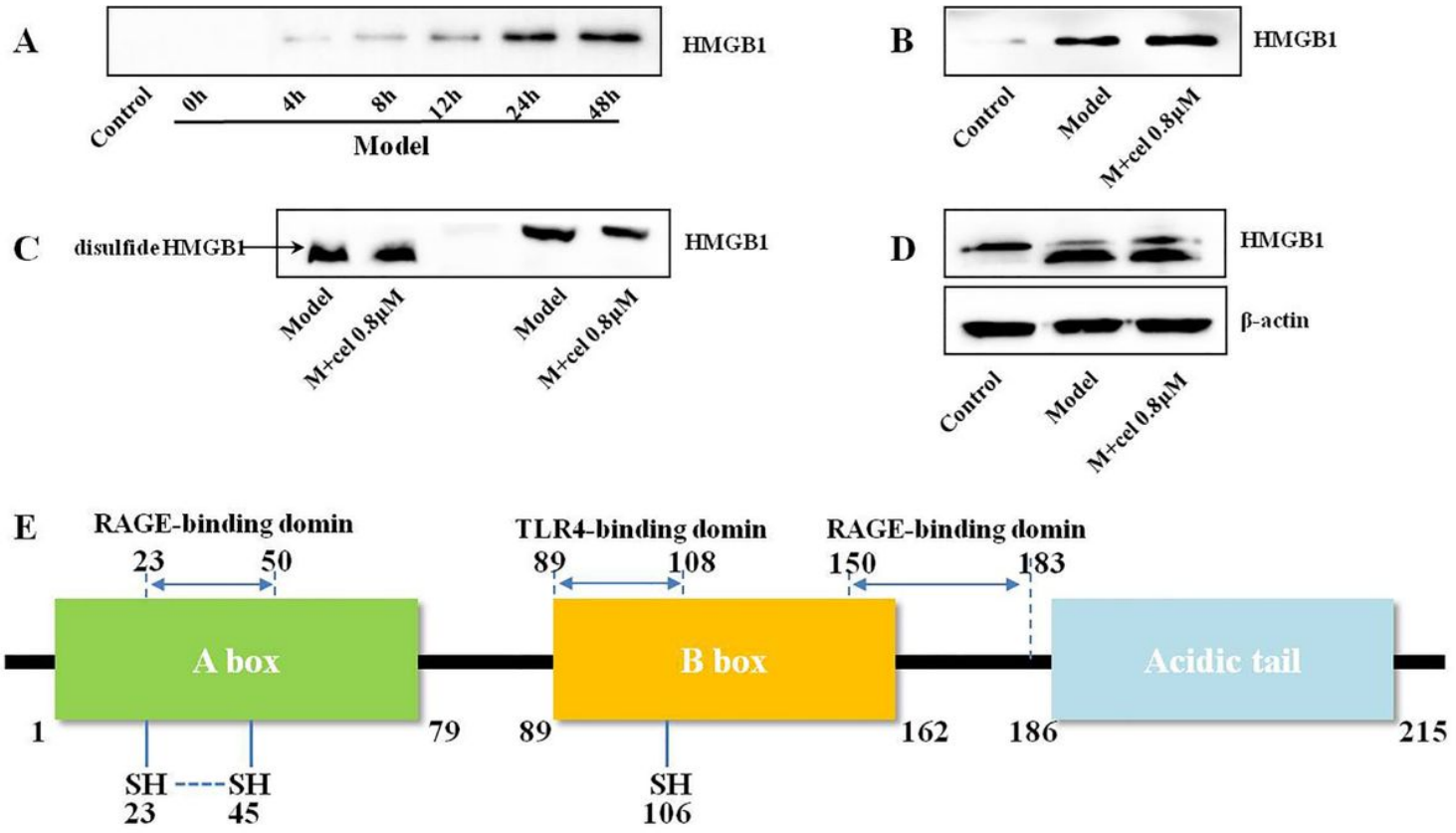

Figure 6

(A) The secreted HMGB1 in OGD model group supernatant medium evolved with time, and reached peak at 24 h. (B) Celastrol did not affect the level of secreted HMGB1 in supernatant medium 48 h after OGD injury. The disulfide but not reduced form HMGB1 occupied the vast majority form of HMGB1 in OGD supernatant (C) and neuron cells (D), and celastrol did not affect the redox state of HMGB1. (E) Structure and function of HMGB1, a 25-kDa protein of 214 amino acids.

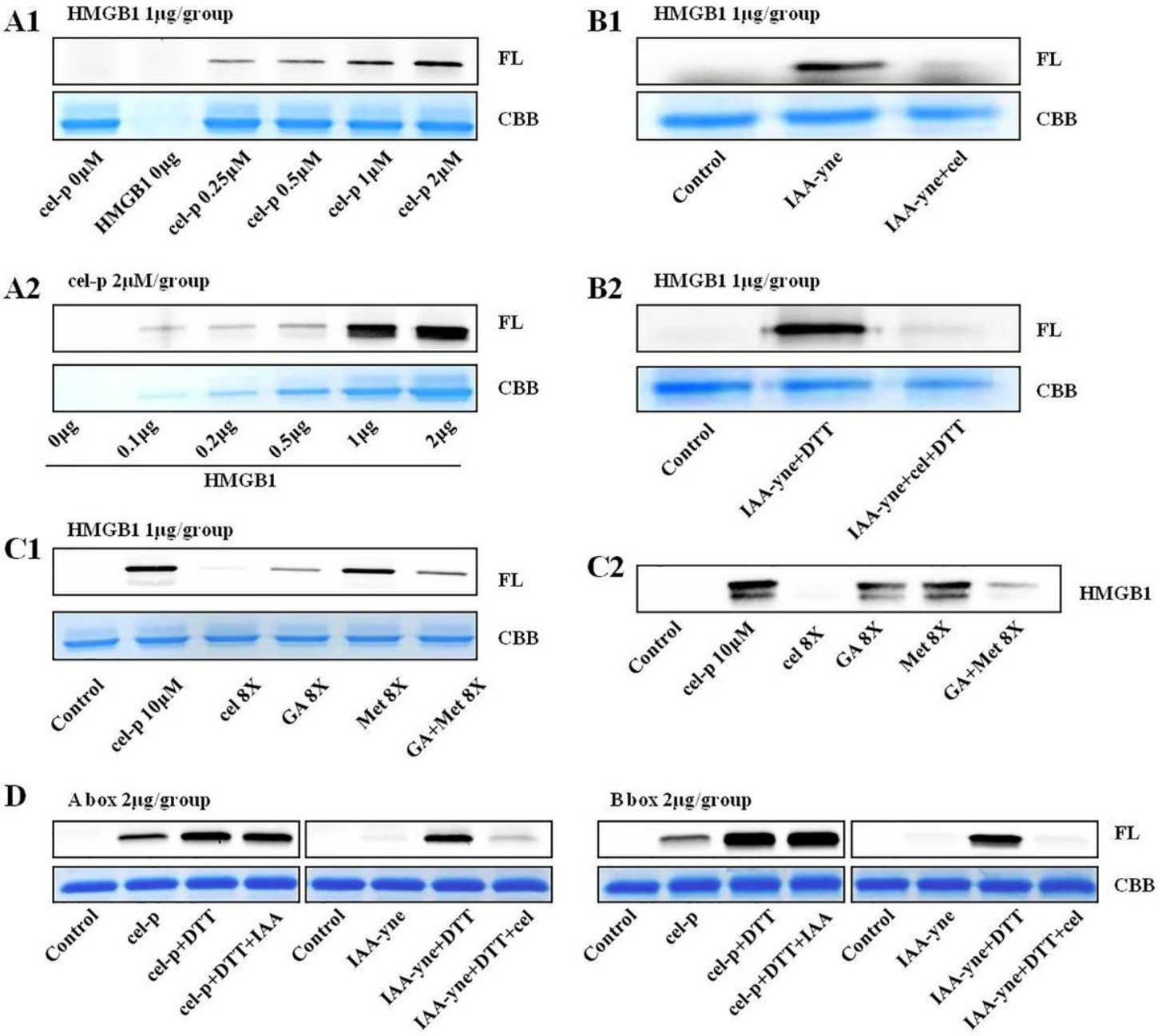

Figure 7

(A-B) Celastrol exhibited strong combining ability with HMGB1 protein in a concentration dependent manner. (C-D) Celastrol almost completely competed the binding of IAA-yne with HMGB1 or DTT reduced HMGB1. (E-F) The binding ability of celastrol to HMGB1 protein was stronger than GA and Metformin. (G) Celastrol could bind to other sites of HMGB1 in addition to the cysteine 23, 45 and 106.

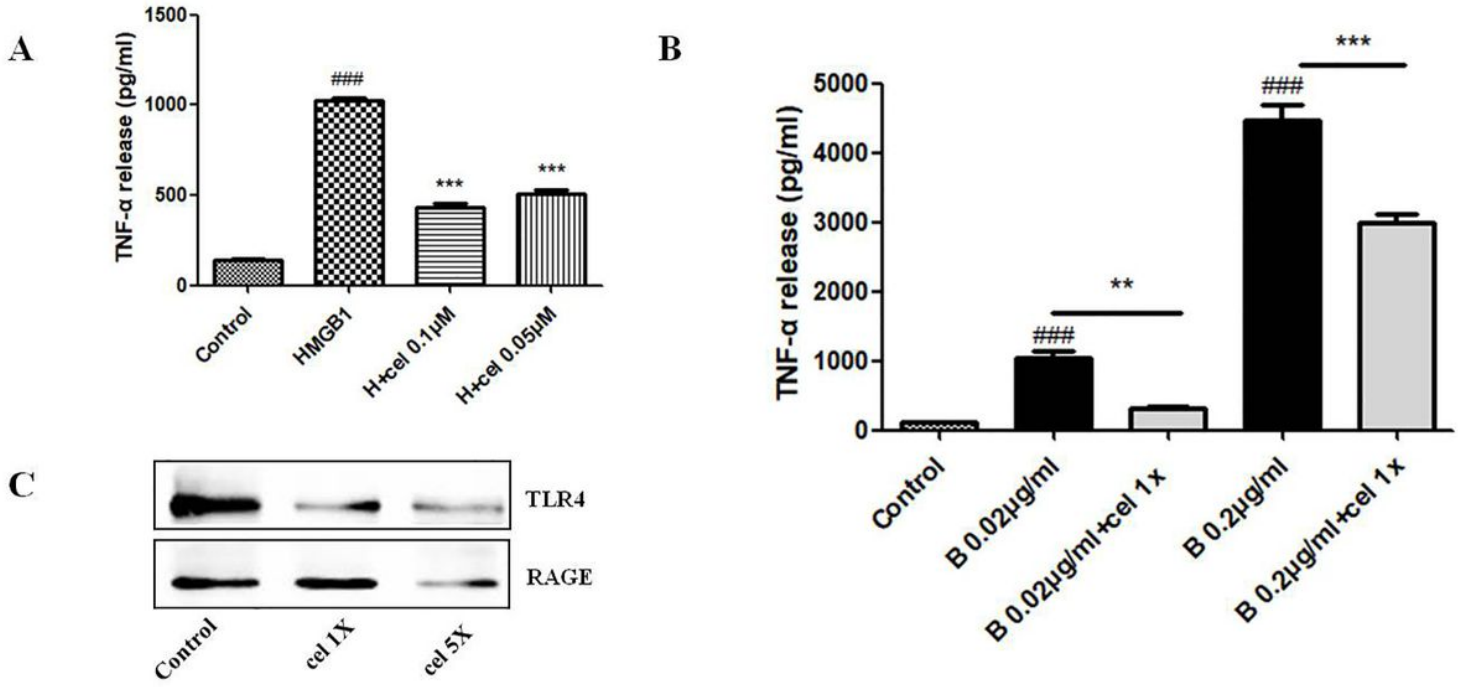

Figure 8

(A) Celastrol significantly inhibited the secretion of TNF-α induced by HMGB1 in RAW 264.7 cells. (B) Celastrol obviously decreased the secretion of TNF-α induced by B box in RAW 264.7 cells. (C) Celastrol remarkable blocked the binding of receptors TLR4 and RAGE to B box. ###p<0.001 vs. Control group, **p 0.01, ***p<0.001 vs. HMGB1 or B box group, One-way analysis of variance was used (n=3).

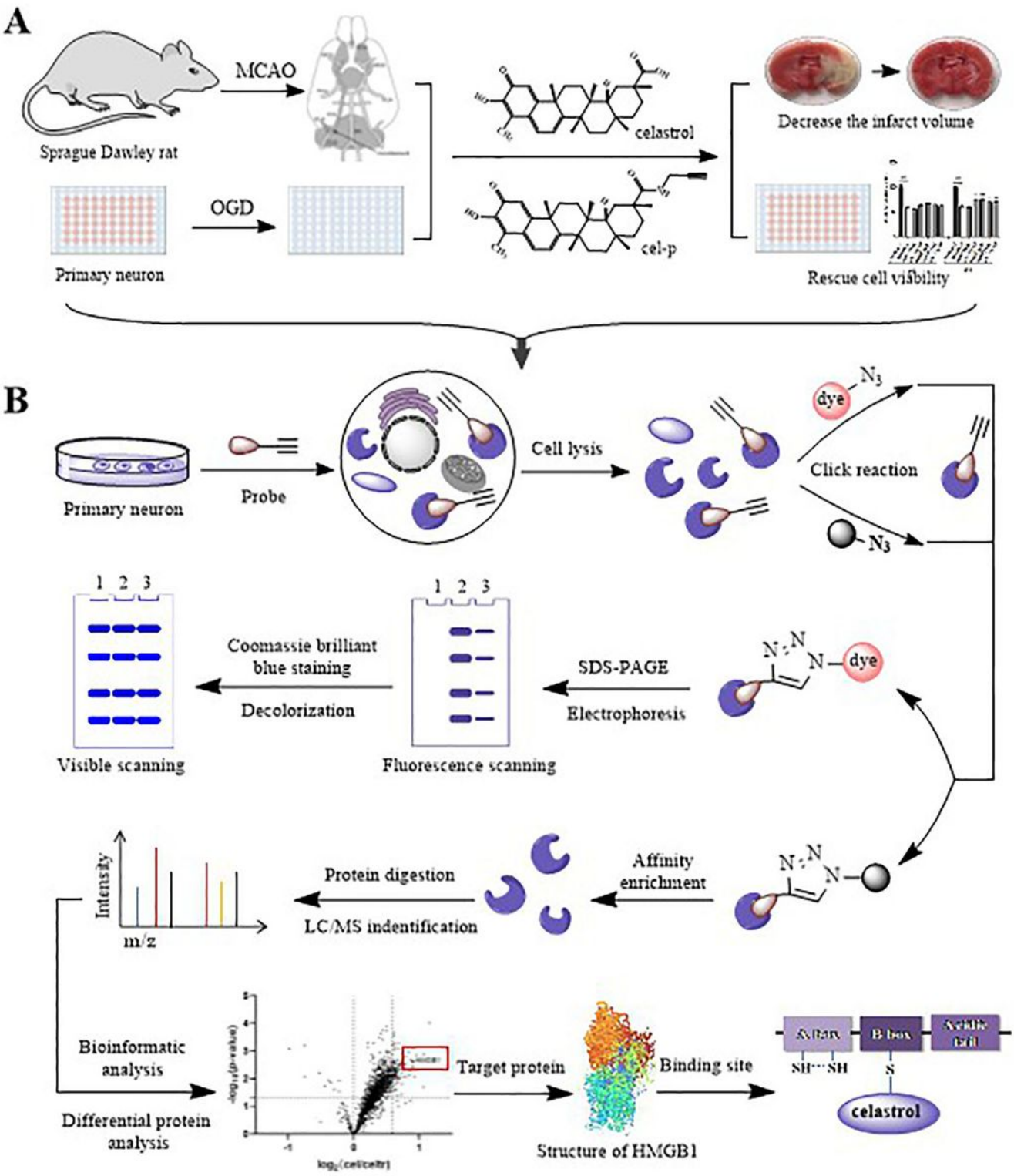

Figure 9

(A) We established OGD model of primary neurons and MCAO model of adult rats to prove that celastrol had neuroprotective effect, and cel-p retained the biological activity of celastrol. (B) We verified HMGB1 as an important target that directly bond by celastrol based on biorthogonal reaction, TMT labeling, LC-MS/MS and CETSA. Celastrol played anti-inflammatory effect by targeting HSP70 and NF-κB and did not

affect the expression changes of HMGB1. Celastrol blocked the cytokines activity of HMGB1 and B box by directly binding them to disrupt the binding of them with inflammatory receptors.

Supplementary Files

This is a list of supplementary files associated with this preprint. Click to download.

- SupplementaryTableS1.xlsx